Electrospinning of 1D Fiber-Like Block Copolymer Micelles with a Crystalline Core

Charlotte E. Ellis, Christian Hils, Alex M. Oliver, Andreas Greiner,* Holger Schmalz,* and Ian Manners*

Electrospinning is a simple, low-cost, and high throughput technique that allows for the processing of polymers into fibers. The process can be controlled to allow access for well-defined continuous fibers that are of interest for a wide range of applications including as tissue scaffolds, as nanowires in optoelectronic devices, and in catalysis. Conventional electrospinning processes use polymer solutions with high molecular weights. Here, the electrospinning of 1D fiber-like block copolymer micelles containing a crystalline core is reported. The successfully accessed core-shell microfibers in which 1D micelles containing a crystalline poly(ferrocenyldimethylsilane) (PFS) core are immobilized on a polystyrene microfiber via coaxial electrospinning. Furthermore, efforts to extend this approach to the use of 1D micelles comprising of a crystalline, π-conjugated poly(di-*n*-hexylfluorene) (PDHF) core are described. Electrospinning is also successfully used to prepare microfibers consisting solely of 1D micelles with a PFS crystalline core, the first examples where a template material is not required.

C. E. Ellis, A. M. Oliver, I. Manners
Department of Chemistry
University of Victoria
Victoria, BC V8P 5C2, Canada
E-mail: imanners@uvic.ca
C. Hils, A. Greiner, H. Schmalz
Macromolecular Chemistry II
University of Bayreuth
95440 Bayreuth, Germany
E-mail: greiner@uni-bayreuth.de; holger.schmalz@uni-bayreuth.de
C. E. Ellis, A. M. Oliver
School of Chemistry
University of Bristol
Bristol BS8 1TS, UK
A. Greiner, H. Schmalz
Bavarian Polymer Institute
University of Bayreuth
95440 Bayreuth, Germany
I. Manners
Center for Advanced Materials and Related Technology (CAMTEC)
University of Victoria
3800 Finnerty Rd, Victoria, BC V8P 5C2, Canada

1. Introduction

The solution self-assembly of amphiphilic block copolymers (BCPs) has been recognized as a valuable bottom-up approach to yielding a vast range of micelle morphologies including spheres, worms, lamellae, and vesicles.[1,2] In particular, 1D micelles are of considerable interest in fields such as catalysis,[3,4] optoelectronics,[5,6] and nanomedicine.[7–13] Non-spherical nanostructures, such as 1D fiber-like micelles, are often challenging to access via the self-assembly of BCPs with amorphous cores as these morphologies with low interfacial curvature typically only exist in restricted regions of the phase space.[2] In the self-assembly of BCPs with a crystallizable core-forming block, however, crystallization provides an additional driving force for the formation of 1D micelles.[14] This phenomenon is termed crystallization-driven self-assembly (CDSA). CDSA yields polydisperse micelles with a lack of length control resulting from the slow and random nature of self-nucleation events which overlap with the growth/elongation step.[1] Low dispersity micelles can be accessed by circumventing the spontaneous (homogeneous) nucleation step of CDSA and performing the self-assembly in the presence of preformed seeds, which act as efficient initiators for the growth/elongation step.[15] Seed micelles are prepared through sonication and fragmentation of polydisperse 1D micelles.[16,17] This seeded-growth process is termed "living" CDSA[18,19] and has been achieved using a variety of crystalline core chemistries such as poly(ferrocenyldimethylsilane) (PFS),[1,15,20] poly(di-*n*-hexylfluorene) (PDHF),[21–23] poly(ε-caprolactone),[24,25] polyethylene,[26,27] and poly(*p*-phenylenevinylene) and related materials.[28–30]

Recent advances have led to further developments of CDSA protocols which have allowed for the upscaled production of 1D micelles with crystalline cores, to help realize their potential applications.[31–35] For example, a process termed polymerization-induced CDSA (PI-CDSA) whereby the BCP synthesis and self-assembly occur in situ allows access to 1D micelles at up to 25 wt%.[31,32] As a result of the diverse range of crystalline core and coronal chemistries compatible with CDSA protocols, 1D micelles prepared using these methods are of interest for a wide range of applications.

Electrospinning is a simple, low-cost, and high throughput method for fabricating continuous fibers with inherently high

**ADVANCED
SCIENCE NEWS**

www.advancedsciencenews.com

{M}acro-
olecular
Chemistry and Physics

www.mcp-journal.de

surface-to-volume ratios.[36–39] The electrohydrodynamic phenomenon depends on a complex interplay of factors such as surface tension, viscosity, and electrical charge.[36] These factors interact in various ways to affect the electrified jet of polymer solution which is ejected from the electrospinning nozzle.[36] Examples of electrospinning high molecular weight polymer solutions are ubiquitous, however, the concept has recently been extended to supramolecular assemblies and crystallizable block copolymers.[40,41]

Coaxial electrospinning is a process that employs a specialized-designed core-shell nozzle containing distinct core and shell solutions for electrospinning.[3,42–46] High molecular weight polystyrene (PS) is often employed as the core since fibers can be easily accessed and optimized, allowing for facile templating of the shell material. When a voltage difference is applied between the collector plate and the nozzle, the solutions are drawn out to form fibers with a core-shell structure. This technique is a cost-effective and high throughput method of processing and preparing fibers for use in devices.[3,47,48] Electrospun and coaxially electrospun fibers have various applications such as in biomedical engineering as tissue scaffolds,[49–51] or in optoelectronics as nanowires.[41,52]

One of our groups and also others have previously demonstrated that coaxial electrospinning can be used to prepare polystyrene microfibers with a sheath of 1D polyethylene-core micelles,[3,43,45,53] yet the scope has not been extended beyond this crystalline core chemistry. Herein, we explore the electrospinning of a variety of different 1D fiber-like micelles by both coaxial and conventional electrospinning methods to access microfibers either exhibiting a core-shell structure or consisting solely of 1D micelles, respectively.

2. Results and Discussion

2.1. Coaxial Electrospinning of PFS-Based 1D Micelles with PS

Coaxial electrospinning allows for the preparation of core-shell microfibers and assists the electrospinning of materials by using a carrier, most commonly high molecular weight PS (**Scheme 1**). The use of a carrier or template is of significant importance for the electrospinning of materials that would typically form particles by "electrospraying".[3,45] BCP micelles generally form electrosprayed particles in electrospinning processes,[54] leading to several challenges in the preparation of fibers containing these nanostructures. Therefore, high molecular weight PS ($M_n = 1.4 \times 10^6$ Da) was employed as the carrier in this work, since this polymer forms well-defined fibers without "beading" (Figure S1, Supporting Information).[3,45] The chemical structures of all BCPs utilized in this study are shown in Figure S2.

We first investigated the coaxial electrospinning of polydisperse PI_{192}-b-PFS_{27} 1D micelles (PI = polyisoprene, indices correspond to number average degree of polymerization of the respective block) which were prepared via PI-CDSA ($L_n = 500–3000$ nm, $W_n = 9 \pm 1$ nm, Figure S3a, Supporting Information).[31,32] For use as the shell, a dispersion of PI_{192}-b-PFS_{27} micelles (2.8 wt% in 20 vol% THF/hexanes; THF = tetrahydrofuran) was prepared. The electrospinning jet was extremely stable under the conditions studied (Table S1, Supporting Information) resulting in the production of well-defined microfibers with relatively monodis-
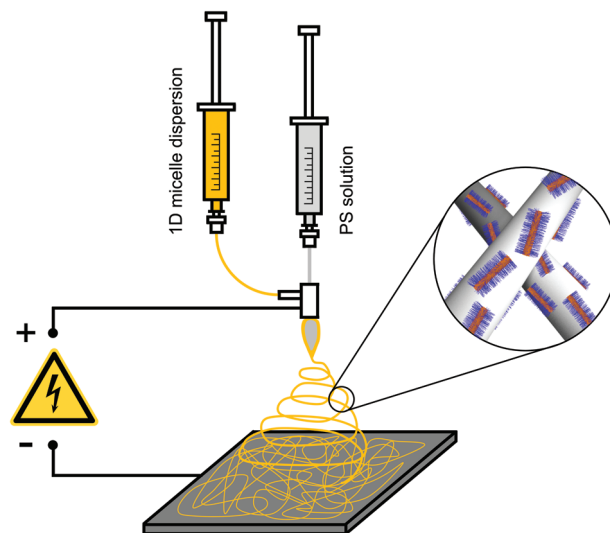
Scheme 1. Preparation of core-shell microfibers by coaxial electrospinning of PS (core, grey) and dispersion of 1D micelles (shell, orange).

perse widths (**Figure 1**). Adhesion of 1D polydisperse micelles to the PS fiber surface was detected by SEM (Figure 1c). Generally, long micelles that are oriented along the long axis of the core PS fiber were observed. However, some short (ca. 100 nm) micelles were also discerned, indicating that some fragmentation may have occurred during the coaxial electrospinning process. The preferred orientation along the long axis of the fiber is presumably a result of shear forces during the electrospinning process.[3,45]

To further characterize the microfibers prepared via coaxial electrospinning, and to determine the coverage of PI_{192}-b-PFS_{27} micelles on the PS fiber surface, Raman spectroscopy was performed (**Figure 2**). The PI_{192}-b-PFS_{27} micelles were found to be dispersed evenly over the PS fiber surface by Raman imaging (Figure 2c). This is supported by the presence of specific bands at Raman shifts of 316 and 1645 cm^{-1} in the respective Raman spectrum extracted from the imaging data (Figure 2e, red spectrum), which can be clearly assigned to the PI_{192}-b-PFS_{27} micelles (Figure 2e, green spectrum). It is noted that due to the smaller diameter of the micelles compared to that of the excited confocal volume, the micelle spectrum is always superimposed with the PS spectrum. Accordingly, on the surface of the coaxially spun fibers, a mixed PS/PI_{192}-b-PFS_{27} micelle phase is detected by Raman imaging (Figure 2c,e).

To further investigate the behavior of PFS-based micelles in coaxial electrospinning, we repeated the procedure using micelle dispersions containing BCPs with different corona-forming blocks, ran-PI_{124}/$PtBS_{125}$-b-PFS_{37} (ran-PI/PtBS = random copolymer of isoprene and 4-$tert$-butylstyrene), Figure S3b, Supporting Information) and $PtBS_{257}$-b-PFS_{38} (Figure S3c, Supporting Information), while keeping the corona-to-core block ratio constant (ca. 7:1). Under the conditions studied (Table S1, Supporting Information), microfibers akin to those when using PI_{192}-b-PFS_{27} micelles were afforded (Figure S4, Supporting Information). However, the 1D micelles were not clearly discernible by SEM analysis (Figure S4b,d, Supporting Information). The microfibers obtained when using ran-PI_{124}/$PtBS_{125}$-b-PFS_{37}
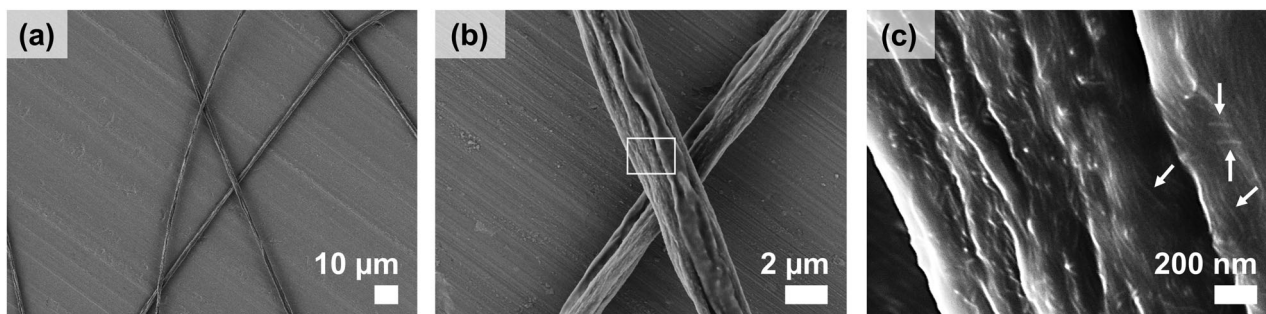
**ADVANCED
SCIENCE NEWS**

www.advancedsciencenews.com

**[M] acro-
molecular
Chemistry and Physics**

www.mcp-journal.de

Figure 1. a) Low magnification and b,c) high magnification SEM images of microfibers prepared via coaxial electrospinning of 1D PI_{192}-b-PFS_{27} micelles (2.8 wt% in 20 vol% THF/hexanes, shell) with PS (7 wt% in dimethylformamide (DMF), core). The inset box on (b) shows the location of the c) high magnification image. Arrows depict the adhesion of 1D PI_{192}-b-PFS_{27} micelles to the PS core fiber. Micelles can be observed over the whole PS fiber surface. Scale bars = 10 µm, 2 µm, and 200 nm were stated.
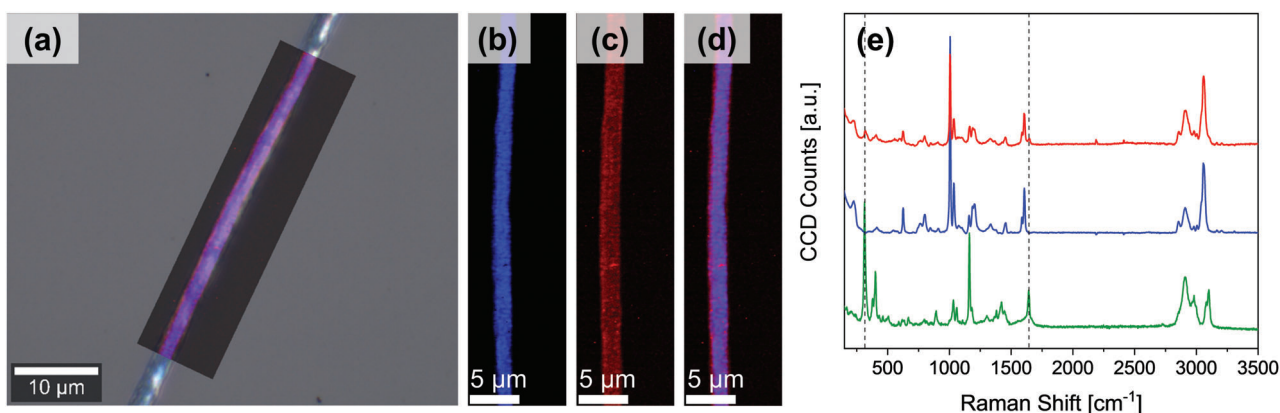

Figure 2. a) Overlay of optical microscopy image with component distribution from Raman imaging for a microfiber prepared via coaxial electrospinning of PI_{192}-b-PFS_{27} micelles (2.8 wt% in 20 vol% THF/hexanes, shell) with PS (7 wt% in DMF, core). Polystyrene-rich areas are colored in blue b) and PI_{192}-b-PFS_{27} rich in red c), respectively. Consequently, mixed phases in the combined distribution d) appear purple. e) Raman spectra of PS (blue) and the mixed PS/PI_{192}-b-PFS_{27} micelle phase (red) derived from true component analysis. In addition, the spectrum of neat PI_{192}-b-PFS_{27} micelles measured separately is displayed in green for comparison. In the Raman spectrum of the mixed PS/PI_{192}-b-PFS_{27} micelle phase, the characteristic peaks at $\tilde{U} = 316$ and 1645 cm^{-1} (indicated by dashed lines) prove the presence of the PI_{192}-b-PFS_{27} micelles.

micelles or $PtBS_{257}$-b-PFS_{38} micelles as the shell solution also exhibited a texture and morphology more similar to that of PS microfibers prepared via conventional electrospinning processes (Figure S1c, Supporting Information).[3] This indicates that coaxial electrospinning was ineffective under these conditions. This could be due to the corona-forming segments, ran-PI_{124}/$PtBS_{125}$ and $PtBS_{257}$, exhibiting more PS-character than that of PI_{192}, causing the core and shell solutions to partially mix upon drying of the electrospinning jet during the course of coaxial electrospinning and deposition on the collector. This could lead to the fiber-like micelles being buried in the PS fiber due to greater coronal compatibility, preventing the formation of a core-shell fiber.

2.2. Extension of Coaxial Electrospinning Approach to $PDHF_{17}$-b-$P2VP_{250}$ 1D Micelles with PS

The emergence of 1D nanoparticles based on BCPs with a π-conjugated crystalline core has led to considerable interest in their application as nanowires in devices.[6,55–57] In this work, our attention turns to the use of 1D micelles containing a PDHF crystalline core prepared via CDSA.[21] Long-range exciton transport

(> 200 nm) that is far superior to that of thin-films of conjugated polymers has been achieved for PDHF-containing nanofibers, owing to the highly ordered crystalline core.[21] Recent studies have further demonstrated the promise of π-conjugated polymer nanofibers containing the donor PDHF crystalline core for optoelectronic applications,[22] such as energy-funneling which enabled a four-fold enhancement of quantum rod emission.[23]

It has been demonstrated that the alignment of 1D micelles with a π-conjugated poly(3-hexylthiophene) crystalline core can greatly enhance charge-carrier mobility.[57] In electrospinning processes, shear forces are exerted on the solution as it passes through the needle, causing BCP micelles to align along the long axis of the resulting fiber.[3] This phenomenon was demonstrated in the coaxial electrospinning of PI_{192}-b-PFS_{27} micelles (Figure 1c) as well as in previous work.[3,45] We were therefore interested in exploring the potential alignment of PDHF-containing micelles with the ultimate future aim of preparing electroactive fibers.

We studied the coaxial electrospinning of $PDHF_{17}$-b-$P2VP_{250}$ 1D micelle (L_n = ca. 2600 nm, P2VP = poly(2-vinylpyridine), Figure S5, Supporting Information) dispersions (1.0 wt% in

ADVANCED
SCIENCE NEWS
www.advancedsciencenews.com

⎰M⎱ acro-
‾‾‾‾ olecular
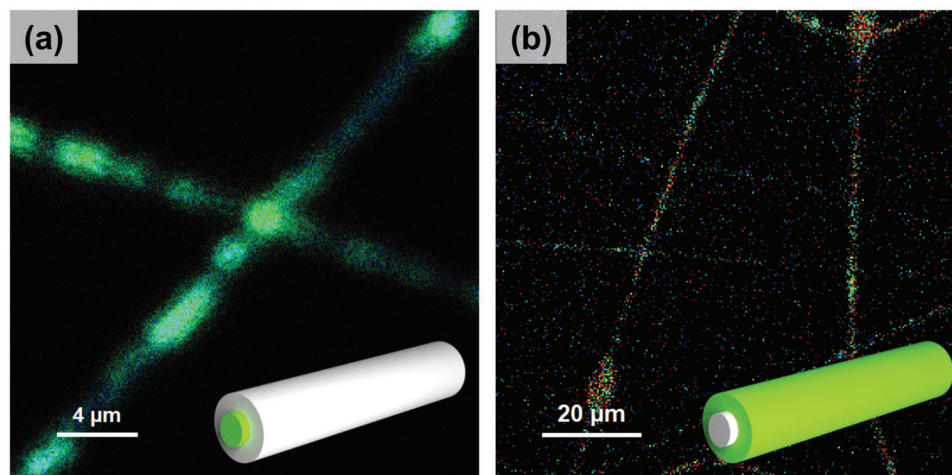Chemistry and Physics
www.mcp-journal.de

Figure 3. Confocal fluorescence microscope images of microfibers prepared via coaxial electrospinning of PDHF$_{17}$-*b*-P2VP$_{250}$ 1D micelles (1.0 wt% in 25/25/50 vol% THF/MeOH/DMSO) with PS (7 wt% in DMF) in which the micelles form a) the core or b) the shell of the fiber. Inset are representations of the core-shell microfiber structure composed of PS (grey) and PDHF$_{17}$-*b*-P2VP$_{250}$ micelles (green). Scale bars = 4 and 20 µm where stated.
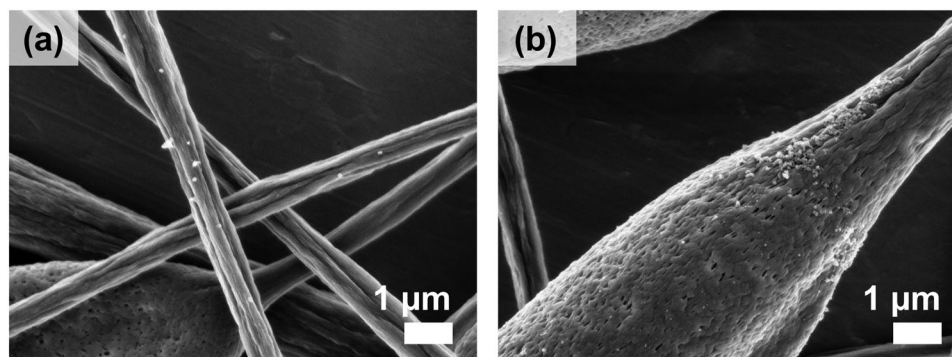

Figure 4. High magnification SEM images of microfibers a) fiber surface and b) beading formed via coaxial electrospinning of PDHF$_{17}$-*b*-P2VP$_{250}$ 1D micelles (1.0 wt% in 25/25/50 vol% THF/MeOH/DMSO, shell) with PS (7 wt% in DMF, core). Scale bars = 1 µm.

25/25/50 vol% THF/MeOH/DMSO; MeOH = methanol, DMSO = dimethyl sulfoxide) with PS ($M_n = 1.1 \times 10^6$ Da, 7 wt% in DMF) as a carrier material. The PDHF$_{17}$-*b*-P2VP$_{250}$ 1D micelles were employed as either the core (**Figure 3**a) or shell (Figures 3b and 4) of the coaxially electrospun fiber. The conditions of the coaxial electrospinning experiments were optimized to stabilize the jet formation and yield fibers with minimal beading (Table S2, Supporting Information). Fluorescence images indicated a relatively even distribution of PDHF$_{17}$-*b*-P2VP$_{250}$ micelles throughout the core (Figure 3a) and shell (Figure 3b) of the coaxially electrospun fibers, compared with a drop-cast micelle dispersion (Figure S6, Supporting Information). On closer inspection, SEM analysis indicated that large populations of micelles exist as beads rather than being evenly distributed over the fiber surface when the micelles were used as shell material (**Figure 4**b). Beading of fibers results from various factors including low solution viscosity, the high net charge density of the jet, and high surface tension.[58] Moreover, the polar P2VP corona of the micelles is not compatible with the non-polar PS carrier fiber, presumably limiting access to uniform fibers via coaxial electrospinning and instead resulting in bead formation. There was not sufficient evidence from SEM analysis to determine whether the PDHF$_{17}$-*b*-P2VP$_{250}$

micelles aligned during the coaxial electrospinning process, as individual 1D micelles could not be identified.

2.3. Electrospinning of PI$_{192}$-b-PFS$_{27}$ 1D Micelles

With the aim of developing microfibers formed exclusively of fiber-like BCP micelles, without the use of a template polymer, electrospinning of PI$_{192}$-*b*-PFS$_{27}$ 1D micelle dispersions was investigated. As previously mentioned, BCP micelle dispersions typically form particles by electrospray in conventional electrospinning procedures,[54] as a result of the many parameters and conditions which require optimization to produce well-defined fibers. We began by exploring the electrospinning of polydisperse PI$_{192}$-*b*-PFS$_{27}$ micelles ($L_n = 500$–3000 nm,) prepared by PI-CDSA at various concentrations (5–20 wt%) in 20 vol% THF/hexanes (Figure S3a, Supporting Information).[31,32] Electrospinning experimental parameters are detailed in Table S3, Supporting Information.

At lower concentrations (≤ 10 wt%), electrospraying of the 1D micelle dispersions was observed (**Figure 5**a,b), resulting in almost exclusively particle formation. This is likely a result of the
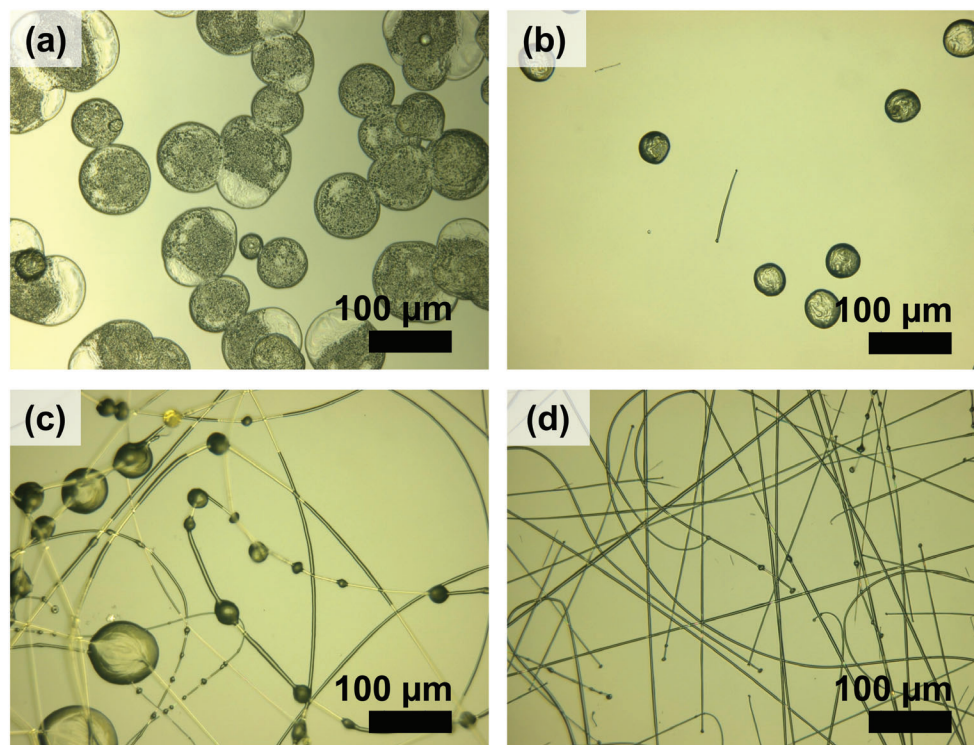
**ADVANCED
SCIENCE NEWS**

www.advancedsciencenews.com

acro-
olecular
Chemistry and Physics

www.mcp-journal.de

Figure 5. Optical microscope images of structures formed via electrospinning of PI_{192}-b-PFS_{27} 1D polydisperse micelle dispersions in 20 vol% THF/hexanes at a) 5 wt%, b) 10 wt%, and c,d) 20 wt% formed at the c) centre, and d) edge of the substrate. Scale bars = 100 μm.

low viscosity of the micelle dispersions at these concentrations preventing electrospinning.[54] At 5 wt%, large particles of diameter 76 ± 26 μm were obtained. On increasing the dispersion concentration to 20 wt%, however, a mixture of fibers and particles was detected (Figure 5c,d). Interestingly, on the edge of the electrospinning substrate, the formation of short fibers dominated that of particles (Figure 5d). Although these results were promising, further optimization was required to access longer continuous electrospun fibers as well as to minimize beading.

Since fiber formation was favored at increased concentration, we looked to further optimize electrospinning conditions using micelle dispersions at high concentrations of 16–20 wt%. First, electrospinning of the polydisperse 1D micelles ($L_n = 500$–3000 nm) at 20 wt% was performed at lower voltages (Figure S7 and Table S3, Supporting Information) with the aim of increasing the stabilization of the jet and promoting improved electrospinning.[59] Fibers were successfully formed via electrospinning, however, the widths varied and some beading was also observed (Figure S7, Supporting Information).

To prevent localized evaporation and therefore minimize beading, a solvent with a higher boiling point (T_b) than the current system, 20 vol% THF/hexanes ($T_b \approx 66$–69 °C), was explored. DMF ($T_b = 153$ °C) has been commonly used as a solvent for the electrospinning of polymeric materials and was therefore employed in this work. However, DMF is a poor solvent for both the PI corona-forming segment and the PFS core-forming segment, meaning only low volume fractions could be studied to prevent precipitation of the micelles. Therefore, micelle dispersions were diluted to 16 wt% with DMF, resulting in a solvent system con-

sisting of 9 vol% DMF and 18 vol% THF in hexanes. Under these conditions (Table S4, Supporting Information), long continuous fibers with relatively monodisperse widths (ca. 3 μm) and the absence of beading were accessed (**Figure 6**). This is likely a result of an increase in the stabilization of the electrospinning jet caused by the presence of DMF, which increases the boiling point of the solvent system. Although individual fiber-like micelles could not be discerned on the microfiber surface by SEM (Figure 6d), we performed a control experiment whereby PI_{273} homopolymer was electrospun (20 wt% in 10 vol% DMF/hexanes) to investigate whether microfibers were formed in the absence of a PFS crystalline core. It was found that, in the absence of 1D PFS crystalline cores, PI_{273} homopolymer did not form electrospun fibers and instead produced particles by electrospraying (Figure S8, Supporting Information). To the best of our knowledge, this work is the first example of electrospun fibers comprising solely of BCP micelles.

It was postulated that the micelle length could also influence the structures obtained via electrospinning. The polydisperse PI_{192}-b-PFS_{27} 1D micelles were sonicated for 1 h at 0 °C to fragment the nanostructures and allow for the study of how micelle length affects the electrospinning process. The resulting micelles were analyzed by TEM (Figure S9, Supporting Information) and were determined to have a length (L_n) and length dispersity (L_w/L_n) of $L_n = 71$ nm and $L_w/L_n = 1.25$. On electrospinning of these shorter micelles, similar results were obtained to that of the long polydisperse micelles. Electrospraying dominated at lower concentrations (≤ 10 wt%) (Figure S10a–c) and electrospinning was achieved at 20 wt% (Figure S10d and Table S5,

**ADVANCED
SCIENCE NEWS**
www.advancedsciencenews.com

Macro-
Molecular
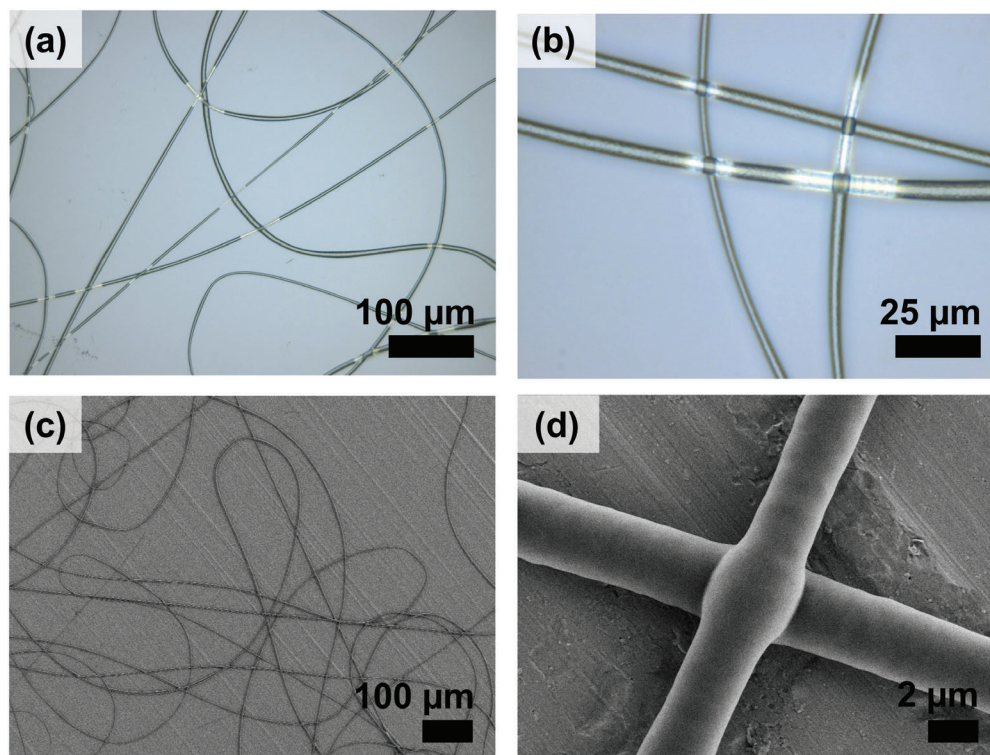Chemistry and Physics
www.mcp-journal.de

Figure 6. a) Low magnification and b) high magnification optical microscope images and c) low magnification and d) high magnification SEM images of microfibers formed via electrospinning of PI_{192}-b-PFS_{27} 1D polydisperse micelle dispersions in 9 vol% DMF and 18 vol% THF in hexanes at 16 wt%. Scale bars = 2, 25, or 100 μm where stated.

Supporting Information for experimental details). The particles formed via electrospraying exhibited diameters with low dispersity. At 5 and 7.5 wt%, the particles had comparable diameters of 5.9 ± 1.8 and 7.5 ± 2.0 μm, respectively, whereas at 10 wt% the diameter was significantly larger (59 ± 26 μm). These findings suggest that the entanglement of micelles in solution does not play a dominant role on the structures obtained. Rather, it is likely that the dispersion concentration, and possibly the formation of a stabilizing liquid crystalline phase,[60] play a more significant role in the electrohydrodynamic phenomenon.

Electrospinning of PFS-based micelles with different corona-forming segments was also explored. Dispersions of *ran*-PI_{124}/$PtBS_{125}$-b-PFS_{37} micelles and $PtBS_{257}$-b-PFS_{38} micelles at 10 wt% in 10/10/80 vol% cyclohexane/THF/hexanes were investigated; however, the solution viscosity was too high to obtain any electrospinning results. On dilution to 5 wt%, only electrospraying to form particles was observed, similar to the case of PI_{192}-b-PFS_{27} micelles.[54]

3. Summary

The processing of 1D micelles via electrospinning techniques (coaxial and conventional electrospinning) was investigated. Using coaxial electrospinning, core-shell fibers whereby the shell consisted of polydisperse PFS-based 1D micelles could be obtained. Coaxial electrospinning using PI_{192}-b-PFS_{27} micelles as the shell yielded fibers in which the micelles were clearly discerned on the surface via SEM analysis. Under the optimized

conditions, the electrospinning jet was extremely stable which resulted in the production of well-defined microfibers without beading. Furthermore, Raman imaging also confirmed the even coverage of PI_{192}-b-PFS_{27} micelles on the PS fiber.

The coaxial electrospinning of 1D $PDHF_{17}$-b-$P2VP_{250}$ micelles with a π-conjugated crystalline core was also explored. In this case, fibers containing 1D micelles as either the core or shell could be obtained. However, coaxially electrospun fibers were found to exhibit beading with uneven micelle distribution over the fiber surface, presumably due to the incompatibility of the polar coronal segment and the non-polar PS carrier fiber. Future work will aim to optimize the coaxial electrospinning of $PDHF_{17}$-b-$P2VP_{250}$ 1D micelles to produce well-defined fibers for use in optoelectronic devices.

Conventional electrospinning to produce fibers consisting solely of 1D PI_{192}-b-PFS_{27} micelles was also described. Fibers consisting of either long (L_n = 500–3000 nm) or short (L_n = 71 nm) micelles were obtained at solution concentrations of 20 wt% but required further optimization to avoid beading. The addition of DMF to the micelle dispersion (to make a final concentration of 16 wt%) was found to stabilize the electrospinning process and allow access to well-defined continuous fibers. The detailed mechanism by which the micelles assemble into the fibers by electrospinning is not clear but their ability to form lyotropic liquid crystals, and therefore to potentially align under the conditions used, may be significant.[60] To the best of our knowledge, this is the first example of fibers prepared via electrospinning of BCP micelle dispersions, without the use of a carrier or template.

**ADVANCED
SCIENCE NEWS**

www.advancedsciencenews.com

**Macro-
molecular**
Chemistry and Physics

www.mcp-journal.de

Supporting Information

Acknowledgements

Conflict of Interest

The authors declare no conflict of interest.

Data Availability Statement

The data that support the findings of this study are available in the supplementary material of this article.

Keywords

[1] U. Tritschler, S. Pearce, J. Gwyther, G. R. Whittell, I. Manners, *Macromolecules* **2017**, *50*, 3439.

[2] Y. Mai, A. Eisenberg, *Chem. Soc. Rev.* **2012**, *41*, 5969.

[3] J. Schöbel, M. Burgard, C. Hils, R. Dersch, M. Dulle, K. Volk, M. Karg, A. Greiner, H. Schmalz, *Angew. Chem., Int. Ed.* **2017**, *56*, 405.

[4] J. Tian, Y. Zhang, L. Du, Y. He, X.-H. Jin, S. Pearce, J.-C. Eloi, R. L. Harniman, D. Alibhai, R. Ye, D. L. Phillips, I. Manners, *Nat. Chem.* **2020**, *12*, 1150.

[5] S. Yang, S. Kang, T. Choi, *Nat. Commun.* **2021**, *12*, 2602.

[6] L. R. MacFarlane, H. Shaikh, J. D. Garcia-Hernandez, M. Vespa, T. Fukui, I. Manners, *Nat. Rev. Mater.* **2021**, *6*, 7.

[7] M. Elsabahy, K. L. Wooley, *Chem. Soc. Rev.* **2012**, *41*, 2545.

[8] Z. Ge, S. Liu, *Chem. Soc. Rev.* **2013**, *42*, 7289.

[9] C. Kinnear, T. L. Moore, L. Rodriguez-Lorenzo, B. Rothen-Rutishauser, A. Petri-Fink, *Chem. Rev.* **2017**, *117*, 11476.

[10] J. D. Garcia-Hernandez, S. T. G. Street, Y. Kang, Y. Zhang, I. Manners, *Macromolecules* **2021**, *54*, 5784.

[11] M. C. Arno, M. Inam, A. C. Weems, Z. Li, A. L. A. Binch, C. I. Platt, S. M. Richardson, J. A. Hoyland, A. P. Dove, R. K. O'Reilly, *Nat. Commun.* **2020**, *11*, 1420.

[12] Y. He, J.-C. Eloi, R. L. Harniman, R. M. Richardson, G. R. Whittell, R. T. Mathers, A. P. Dove, R. K. O'Reilly, I. Manners, *J. Am. Chem. Soc.* **2019**, *141*, 19088.

[13] S. T. G. Street, Y. He, X.-H. Jin, L. Hodgson, P. Verkade, I. Manners, *Chem. Sci.* **2020**, *11*, 8394.

[14] J. A. Massey, K. Temple, L. Cao, Y. Rharbi, J. Raez, M. A. Winnik, I. Manners, *J. Am. Chem. Soc.* **2000**, *122*, 11577.

[15] J. B. Gilroy, T. Gädt, G. R. Whittell, L. Chabanne, J. M. Mitchels, R. M. Richardson, M. A. Winnik, I. Manners, *Nat. Chem.* **2010**, *2*, 566.

[16] G. Guerin, H. Wang, I. Manners, M. A. Winnik, *J. Am. Chem. Soc.* **2008**, *130*, 14763.

[17] G. Guerin, P. A. Rupar, M. A. Winnik, *Polymers* **2021**, *13*, 3122.

[18] S. Ganda, M. H. Stenzel, *Prog. Polym. Sci.* **2020**, *101*, 101195.

[19] L. R. MacFarlane, C. Zhao, J. Cai, H. Qiu, I. Manners, *Chem. Sci.* **2021**, *12*, 4661.

[20] X. Wang, I. Manners, M. A. Winnik, *Science* **2007**, *317*, 644.

[21] X. Jin, M. B. Price, J. R. Finnegan, C. E. Boott, J. M. Richter, A. Rao, S. M. Menke, R. H. Friend, G. R. Whittell, I. Manners, *Science* **2018**, *900*, 897.

[22] H. Shaikh, X.-H. Jin, R. L. Harniman, R. M. Richardson, G. R. Whittell, I. Manners, *J. Am. Chem. Soc.* **2020**, *142*, 13469.

[23] Y. Zhang, H. Shaikh, A. J. Sneyd, J. Tian, J. Xiao, A. Blackburn, A. Rao, R. H. Friend, I. Manners, *J. Am. Chem. Soc.* **2021**, *143*, 7032.

[24] M. C. Arno, M. Inam, Z. Coe, G. Cambridge, L. J. Macdougall, R. Keogh, A. P. Dove, R. K. O'Reilly, *J. Am. Chem. Soc.* **2017**, *139*, 16980.

[25] W. Yu, J. C. Foster, A. P. Dove, R. K. O'Reilly, *Macromolecules* **2020**, *53*, 1514.

[26] J. Schmelz, A. E. Schedl, C. Steinlein, I. Manners, H. Schmalz, *J. Am. Chem. Soc.* **2012**, *134*, 14217.

[27] C. Hils, J. Schmelz, M. Drechsler, H. Schmalz, *J. Am. Chem. Soc.* **2021**, *143*, 15582.

[28] S. Shin, F. Menk, Y. Kim, J. Lim, K. Char, R. Zentel, T.-L Choi, *J. Am. Chem. Soc.* **2018**, *140*, 6088.

[29] L. Han, M. Wang, X. Jia, W. Chen, H. Qian, F. He, *Nat. Commun.* **2018**, *9*, 865.

[30] D. Tao, C. Feng, Y. Cui, X. Yang, I. Manners, M. A. Winnik, X. Huang, *J. Am. Chem. Soc.* **2017**, *139*, 7136.

[31] C. E. Boott, J. Gwyther, R. L. Harniman, D. W. Hayward, I. Manners, *Nat. Chem.* **2017**, *9*, 785.

[32] A. M. Oliver, J. Gwyther, C. E. Boott, S. A. Davis, S. Pearce, I. Manners, *J. Am. Chem. Soc.* **2018**, *140*, 18104.

[33] Y. Sha, M. A. Rahman, T. Zhu, Y. Cha, C. W. McAlister, C. Tang, *Chem. Sci.* **2019**, *10*, 9782.

[34] P. J. Hurst, A. M. Rakowski, J. P. Patterson, *Nat. Commun.* **2020**, *11*, 4690.

[35] S. Guan, W. Wen, Z. Yang, A. Chen, *Macromolecules* **2020**, *53*, 465.

[36] D. H. Reneker, A. L. Yarin, *Polymer* **2008**, *49*, 2387.

[37] S. Agarwal, A. Greiner, J. H. Wendorff, *Prog. Polym. Sci.* **2013**, *38*, 963.

[38] A. Greiner, J. H. Wendorff, *Angew. Chem., Int. Ed.* **2007**, *46*, 5670.

[39] T. Tabrizizadeh, J. Wang, R. Kumar, S. Chaurasia, K. Stamplecoskie, G. Liu, *ACS Appl. Mater. Interfaces* **2021**, *13*, 50900.

[40] A. S. Tayi, E. T. Pashuck, C. J. Newcomb, M. T. McClendon, S. I. Stupp, *Biomacromolecules* **2014**, *15*, 1323.

[41] W. Huang, M.-J. Wang, C.-L. Liu, J. You, S.-C. Chen, Y.-Z. Wang, Y. Liu, *J. Mater. Chem. A* **2014**, *2*, 8416.

[42] M. Burgard, D. Weiss, K. Kreger, H. Schmalz, S. Agarwal, H. W. Schmidt, A. Greiner, *Adv. Funct. Mater.* **2019**, *29*, 1903166.

[43] C. Hils, M. Dulle, G. Sitaru, S. Gekle, J. Schöbel, A. Frank, M. Drechsler, A. Greiner, H. Schmalz, *Nanoscale Adv.* **2020**, *2*, 438.

[44] G. Duan, A. Greiner, *Macromol. Mater. Eng.* **2019**, *304*, 1800669.

[45] A. Frank, C. Hils, M. Weber, K. Kreger, H. Schmalz, H.-W Schmidt, *Angew. Chem., Int. Ed.* **2021**, *60*, 21767.

[46] D. Han, A. J. Steckl, *ChemPlusChem* **2019**, *84*, 1453.

[47] Y. Lu, J. Huang, G. Yu, R. Cardenas, S. Wei, E. K. Wujcik, Z. Guo, *Wiley Interdiscip. Rev.: Nanomed. Nanobiotechnol.* **2016**, *8*, 654.

[48] Z. Sun, E. Zussman, A. L. Yarin, J. H. Wendorff, A. Greiner, *Adv. Mater.* **2003**, *15*, 1929.

[49] X. Jing, H.-Y. Mi, X.-C. Wang, X.-F. Peng, L.-S Turng, *ACS Appl. Mater. Interfaces* **2015**, *7*, 6955.

[50] T. Yu, S. E. Gleeson, C. Y. Li, M. Marcolongo, *J. Biomed. Mater. Res., Part B* **2019**, *107*, 1141.

[51] M. Norouzi, S. M. Boroujeni, N. Omidvarkordshouli, *Adv. Healthcare Mater.* **2015**, *4*, 1114.

[52] H. Chen, N. Wang, J. Di, Y. Zhao, Y. Song, L. Jiang, *Langmuir* **2010**, *26*, 11291.

[53] A. Frank, M. Weber, C. Hils, U. Mansfeld, K. Kreger, H. Schmalz, H. Schmidt, *Macromol. Rapid Commun.* **2022**, *43*, 2200052.

[54] L. Wang, P. D. Topham, O. O. Mykhaylyk, H. Yu, A. J. Ryan, J. P. A. Fairclough, W. Bras, *Macromol. Rapid Commun.* **2015**, *36*, 1437.

[55] N. E. Persson, P. H. Chu, M. McBride, M. Grover, E. Reichmanis, *Acc. Chem. Res.* **2017**, *50*, 932.

[56] O. El-Zubir, E. L. Kynaston, J. Gwyther, A. Nazemi, O. E. C. Gould, G. R. Whittell, B. R. Horrocks, I. Manners, A. Houlton, *Chem. Sci.* **2020**, *11*, 6222.

[57] X. Li, P. J. Wolanin, L. R. MacFarlane, R. L. Harniman, J. Qian, O. E. C. Gould, T. G. Dane, J. Rudin, M. J. Cryan, T. Schmaltz, H. Frauenrath, M. A. Winnik, C. F. J. Faul, I. Manners, *Nat. Commun.* **2017**, *8*, 15909.

[58] H. Fong, I. Chun, D. H. Reneker, *Polymer* **1999**, *40*, 4585.

[59] T. Han, A. L. Yarin, D. H. Reneker, *Polymer* **2008**, *49*, 1651.

[60] D. W. Hayward, J. B. Gilroy, P. A. Rupar, L. Chabanne, C. Pizzey, M. A. Winnik, G. R. Whittell, I. Manners, R. M. Richardson, *Macromolecules* **2015**, *48*, 1579.